Asian Journal of Chemistry; Vol. 34, No. 12 (2022), 3108-3114

ASIAN JOURNAL OF CHEMISTRY

https://doi.org/10.14233/ajchem.2022.23860

Phosphonium Grounded Ionic Liquid Influenced in Graphene Oxide Enabled to Magnetic Polysulfone (GO/Fe_3O_4@PSF) for the Elimination of 2,4-Dichlorophenol

M.S. MANOJKUMAR[1,*] and B. SIVAPRAKASH[2]

[1]Department of Biotechnology, Vivekanandha College of Engineering for Women (Autonomous), Namakkal-637205, India
[2]Department of Chemical Engineering, Annamalai University, Annamalai Nagar-608002, India

*Corresponding author: E-mail: msmanojkumar1987@gmail.com

Received: 5 April 2022; *Accepted*: 4 September 2022; *Published online*: 25 November 2022; AJC-21034

The phase separation technique was used to create magnetic polysulfone facilitated to graphene oxide (GO/Fe_3O_4@PSF) entrapped with the phosphonium-based ionic liquid which removes the phenolic content from aqueous medium. Scanning electron microscopy, Brunauer-Emmett-Teller, Fourier transform infrared spectroscopy and thermogravimetric analysis were used to characterize the supplement and the immobilization of trihexyltetradecylphosphonium decanoate as ionic liquid in magnetic polysulfone assisted GO was ascertained to be 83.3%. Adsorbent analysis revealed that the established granules have the ability to remove a wide range of phenolic compounds. The strongest expulsion of 2,4-dichlorophenol (2,4-DCP) has been accomplished among pH 2.0 and 11. At 25-70 ºC had no substantial influences on adsorbent, displaying the adsorbent's suitability for use with genuine effluents. Sorption capacity evidenced that the pathway takes place in second order and the Weber-Morris template constrained the adsorbent limiter as adsorbate molecules. The Redlich-Peterson concept was indeed the great candidate for the experimental evidence, with a significance of 0.82 approaching the Langmuir isotherm model, which also acquired a q_{max} of 404.50 mg/g. As a method of gathering data, these supplements have the great promise to be used in the treatment of phenolic compound caused environmental contamination.

Keywords: Phosphonium ionic liquid, 2,4-Dichlorophenol, Weber Morris model, Langmuir isotherm.

INTRODUCTION

Environmental damage from phenolic elements in aquatic ecosystems encompasses a wide array of sources, including industrial effluents from various sectors, including gasoline, petroleum products, fuel transformation, varnishes, synthetic polymer epoxy and the paper industry [1-4]. Such additives harm the health by adversely impacting the nervous system, digestive tract, eye-lids, cardiovascular system, respiratory system, and spleen, as well as causing toxic effect, histological changes, genotoxicity and carcinogenic effects [5-7].

Effluent containing phenolic compounds should be addressed before it can be used or disposed into accepting waterways. In addition to the inherent substances, use of pesticide 2,4-dichlorophenoxyacetic acid (2,4-D) across many agro based crop production results in the formation of 2,4-dichlorophenol (2,4-DCP) substance during degradation. Unquestionably, there is a significant environmental factor while looking for alternatives to phenolic component reduction approaches. Several methods used to remove these phenolic compounds from the aqueous phase, including disintegration adsorbents, separation and purification, enzyme degradation and photocatalytic degradation [8].

Adsorption is a technique for removing contaminates from aqueous phase. Charcoal, recycled fibers and polyurethanes have mostly been studied as adsorbent materials. The features of these adsorbents are their convenience of separation, uptake capacity and supplemented [9]. Even though, there are huge obstacles, including such intraparticle diffusion strength and inadequate adhesion. Fluid separation, on the other hand, has a high adsorption capability. Polymeric membrane, encapsulating feature extraction methods have been employed to combine multiple areas [10].

Graphene is also being used as an adsorption process inside the basic premise of this methodology, due to its extreme large surface area, outstanding chemical reliability and good thermal stability [11]. The graphene oxide polymeric hybrid catalyst, which had fascinated the attention of many researchers due to

their excellent achievement and wide range of applications [12]. Fe_3O_4/graphene composites, as one category of graphene hybrid material, were used as governed targeted drug carriers [13], toxic elements and colourant separation [14], magnetic resonance imaging [15], *etc*.

Due to their superior chemical and thermal stability, porous structural arrangement in their morphological features, and biocompatibility, polysulfone polymer (PSF) has an advantage in many industries of feedstocks [16]. In order to fully participate, neither the finding of phosphonium-based immobilised in membranes nor the existence of shells has been revealed. As a result, with the goal of incorporating the intriguing features in addition to phenolic compound discharge and the convenience of detachment of polymeric capsules facilitated graphene oxide along magnetite in reactors (GO/Fe_3O_4@PSF), the primary objective of this research has been to immobilize a phosphonium based ionic liquid, trihexyl tetradecyl phosphonium decanoate ([P_{66614}][$C_9H_{19}COO$]), in highly permeable magnetic polysulfone capsules facilitated graphene oxide to appraise the discharge of phenolic compounds in aqueous solution, with a focus on 2,4-dichlorophenol, predicated on the adsorption-desorption assertion.

EXPERIMENTAL

Synthesis of graphene oxide: Augmented graphite was used for the synthesis of graphene oxide using the Hummer's static method. The procedure that was used is as follows: sodium nitrate (0.5 g) and potassium permanganate (0.3 g) were added to 98% sulphuric acid in an ice-cold basket. By constantly stirring, the expanded graphic substances was added and the rate of adding will be at normal so that the temperature will not increase suddenly. The resulted solution was sustained in an ice cube tray at 40 ºC and stored in the refrigerator for over 24 h. Then the obtained result was placed in an oil bath at 350 ºC for 30 min. Following that deionized water was added progressively to the mixture and the temperature was raised up to 98 ºC for over 15 min. Then, 30% H_2SO_4 has added a dropwise under the observing the appearance of bubbles. Then the supernatant was kept aside and washed with 5% HCl and the deionized water is used to dissolve the excess acid. Then the results of substances were air-dried at room temperature.

Graphene oxide assisted with magnetic polysulfone capsules: By using the phase inversion precipitation method, GO/Fe_3O_4@PSF capsules were prepared [17]. In brief, a 15 mL of DMF solution containing polysulfonate capsules were prepared in a dispersed solution using ultrasonication process. Then 10 mg of ferrous oxide nanoparticles was added along with 10 mg of S-IPBA. Then at room temperature, the mixture is mixed well for over 2 h. By mixing the SDS aqueous solution with ethanol, the continuous phase was prepared. In the continuous phase, the dispersed solution was added with the help of a 0.45 mm diameter needle and a cylinder shaped capsule was obtained. And the obtained capsules were separated from the continuous phase with the help of a magnetic stirrer and washed lightly with distilled water and ethanol, 3 times for each capsule and then desiccated at 50 ºC.

Adsorption experiments: The phenolic compound was organized in a reaction mixture containing 50 mg L^{-1}. The supplements were being mixed into 100 mL of sample and continued to keep at 200 rpm for 5 h. The experiment was done in triplicate to estimate the accumulation at the beginning ad at the finish of the test. The number of harmful substances in the adsorption experiment per gram of capsule, as per exponential function:

$$q_e = \frac{(C_o - C_e)V}{M} \quad (1)$$

where q_e = amount of phenolic substances adsorption per gram of capsule; C_o = original concentration of phenolic substances; C_e = steady-state concentration of phenolic substances; V = volume of solution; M = number of capsules.

The influences of solution pH and temperature have been examined in triplicate experimental tests, as well as the procured mean value has been differentiated using a Tukey test. The primed capsules (20 mg) were incubated for 5 h at 200 rpm in the mechanical shaker and then mixed with 2, 4-DCP solution. The evidence gathered in triplicate experimental tests were used to study the adsorption characteristics and isotherm evaluation.

Influence pH of solution: A suspension of 1000 mg L^{-1} of 2,4-DCP was made and afterward separated into individual pieces through the use of fluids containing NaOH and HCl to maintain pH from 2 and 11. A pH meter was used to evaluate the pH. Then an oscillator was held at 21 ºC with 5.0 mL of fluid and 20 mg of capsule.

Influence of temperature: The assessment with the microsphere containing 800 mg L^{-1} 2, 4-DCP was used. The backing temperature has been used in this investigation were 25, 30, 40, 50 and 60 ºC.

Kinetic model of adhesion: To examine the adsorption behaviour, a 1000 mg L^{-1} 2,4-DCP was 30 mL, 125 mg of capsule was applied to measure the quantities of phenol contaminants were assessed at pre-determined time periods in standardized settings is 5 h for 200 rpm at 21 ºC. The variables have been employed to develop pseudo-first and second-order, along with Weber-Morris's kinetics characteristics of adhesion.

Adsorption equilibrium: While dissolving capsule (50, 100, 200 and 300 mg) in 1000 mg L^{-1} 2,4-DCP, the adsorbent has been established (15 mL). For 5 h, the adsorbed procedure was carried out at constant temperatures of 21 ºC, with a pH of 6.50 and agitating at 200 rpm. The equilibrium adsorption modeling Langmuir, Freundlich and Redlich-Peterson have been used. An experiment was performed alone without ionic liquid to investigate the capsules' adhesion in 2,4-DCP solution, which served as an unreadable assay for the capsules.

RESULTS AND DISCUSSION

Morphology: Procured capsules were seen in Fig. 1a, with reliability in morphology and an estimated value size of 2, 74 mm and 0.17 mm, respectively. The SEM micrographs of the capsules either with or without ionic liquid are shown in Figs. 1a and b, respectively. Its first framework in Fig. 1a has a porous structure because when the encapsulated subs-

tance is examined, it has a smoother texture. The image of crosssection can be used to examine the internal morphology. Fig. 1c interprets a plain supplement with high porosity, whereas Fig. 1d depicted the encapsulated substance with morphological characteristics related to the plain capsule, which is fairly close to the encapsulated molecule's core structure, and thus improving the accessibility of the founded porous structure. Other researchers have also reported the similar polysulfone capsule surface characteristics [18].

FTIR studies: Fig. 2a illustrates the infrared spectra of polysulfone capsules revealed characteristic bands at 1636 cm^{-1}. The GO/Fe_3O_4@PSF showed band appears at 2346 cm^{-1} where the C-H stretching of carbonyl groups observed, 1416 cm^{-1} and 1299 cm^{-1} shows stretching vibrations of O–S–O. Hence, the encapsulated substances produced an FT-IR spectral range that was similar to the genuine capsule in Fig. 2b but with an increase in binding affinity of 1416 cm^{-1} of stretching in C–O, 1299 cm^{-1} as stretching mode of P+O, whereas 769 cm^{-1} is the frequency in stretching of P-C [19,20] is also observed.

BET analysis: Fig. 3a proves the approach of ionic liquid immobilization. The exterior region of the encapsulated ionic liquid was 95 times lower than the genuine capsule, indicating that the pore spaces have been filled, which would be responsible for the decrease in the exterior region. This statement was supported by the pore space, which was reduced during the immobilization phase from 0.0751 cm^3g^{-1} to 0.0016 cm^3g^{-1}. And the pore diameter, on the other hand, expanded about twofold, indicating that fairly small pore spaces have been packed during immobilization. The surface area, as per the fiction, is strongly attributable to the adsorption process. Even so, the capsule aspires to comprise the ionic liquid while having performed fluid retrieval, although, with different size relevance, the capsule with immobilization would then perform much better than the genuine capsule [21].

Effect of pH: The effect of pH in the solution is shown in Fig. 4a, upon the adsorbent of 2, 4-DCP toxicant produced by the capsule. It was probable to see that fluid was unfavorable for the adsorption process in an alkaline environment with a pH > 10. This is due to the negative ionic form of 2,4-DCP being ineffective for adsorption; the interparticle hydrogen adhesion among the –OH groups of 2,4-DCP as well as the phosphonium class in ionic liquid. Adsorbent surface volumes for them were comparable to 220 mg L^{-1}, which was still nearer to some other mean values, which attained around 240 mg L^{-1}. One such decrease could be attributed to the high electron at the studied pH values [22].

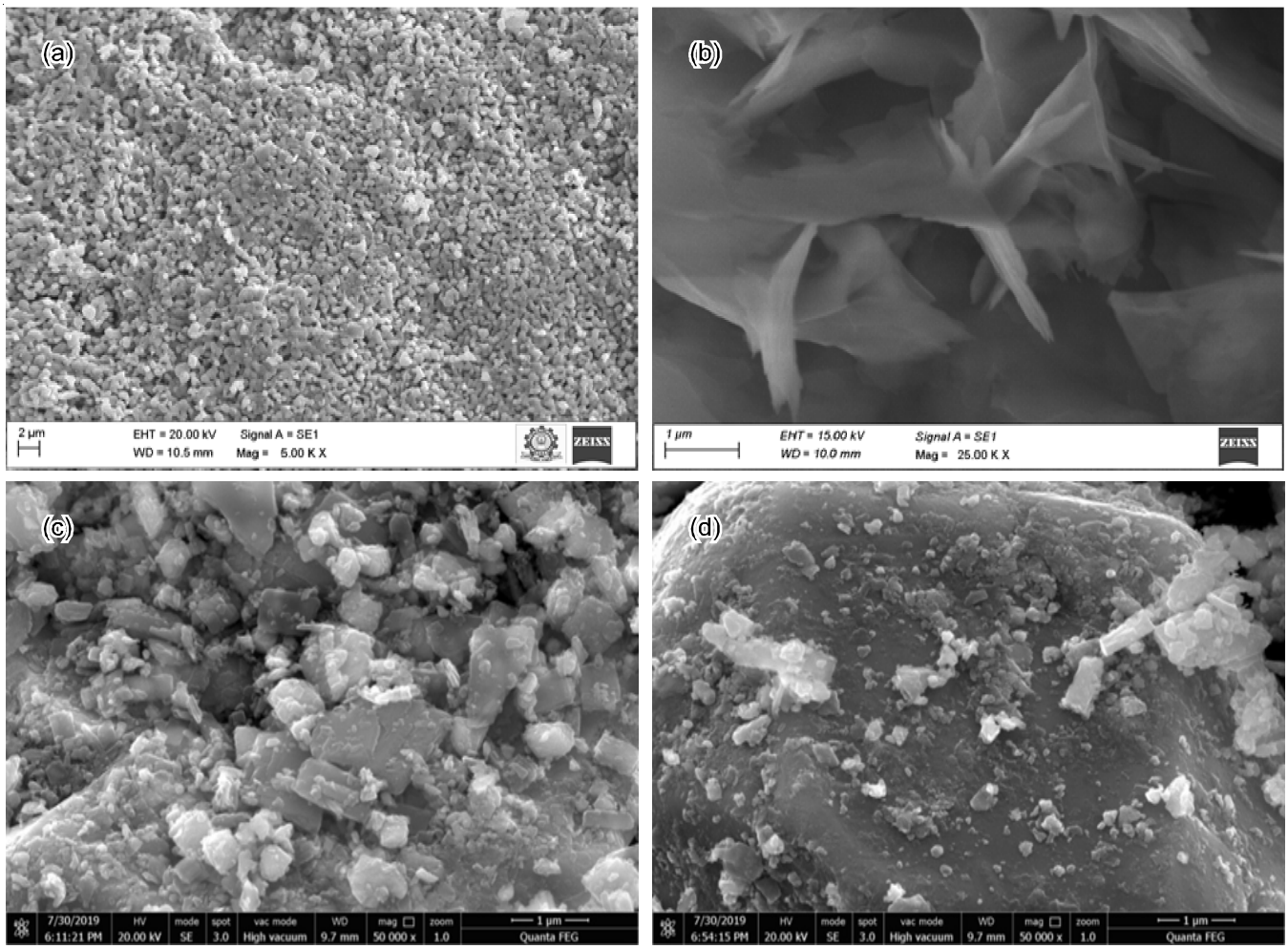

Fig. 1. SEM profile (a) polysulfone capsules, (b) graphene oxide/polysulfone, (c) graphene oxide/c, (d) graphene oxide/Fe_3O_4@polysulfone capsules

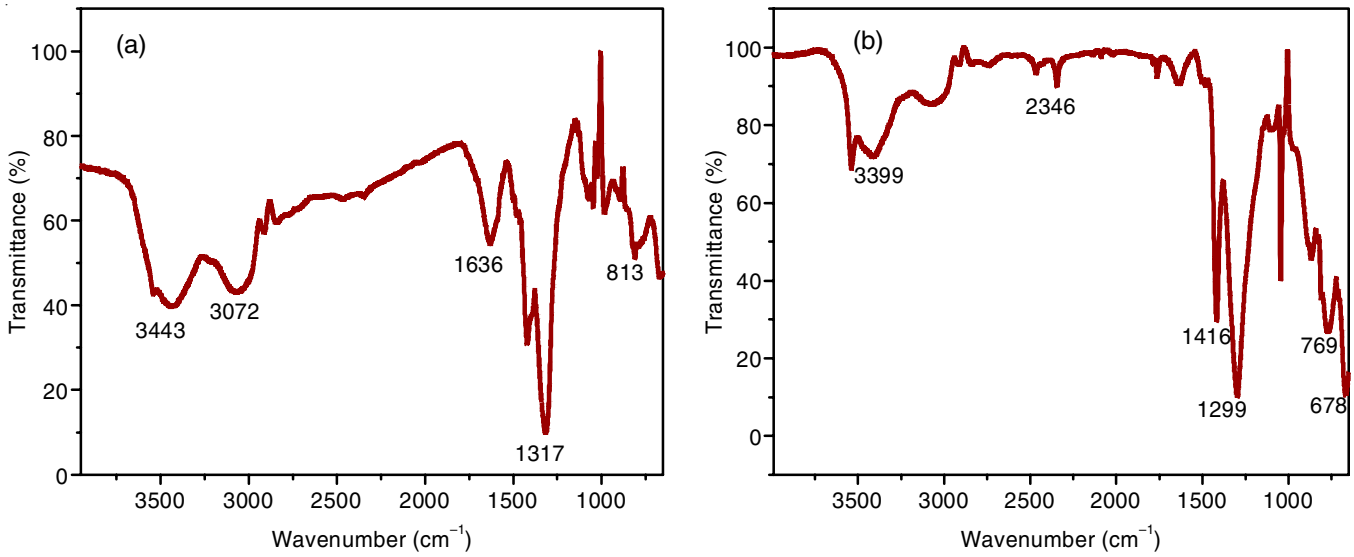

Fig. 2. (a) FTIR spectrum of poly-sulfone capsules (b) graphene oxide incorporate magnetic polysulfone capsules

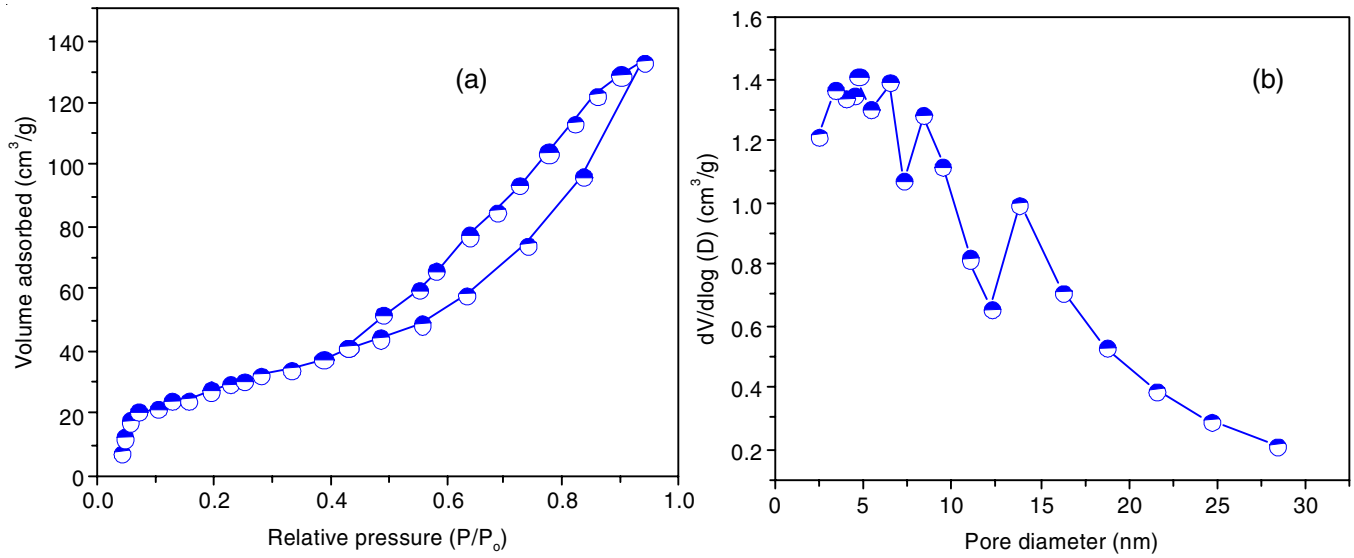

Fig. 3. (a) BET isotherm spectra (b) pore volume *vs*. pore diameter of graphene oxide incorporate magnetic polysulfone capsules

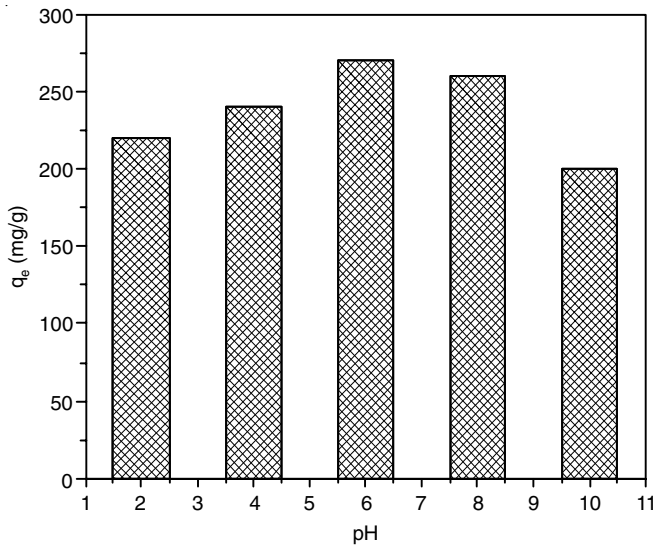

Fig. 4a. Effect of pH containing 2,4-DCP concentration

Effect of temperature: Fig. 4b shows that no substantial variations in the adsorbent's mean values have been observed, exhibiting the validity of the system to polysulfone capsules in the range of temperature described. Since, when statistics are linearly regressed, the curve coefficient is lower, indicating that indeed greater the surface temperature, the lesser the quantity of charge in the capsules. It also demonstrated that the adsorption process is exothermic in nature.

Adsorption kinetics: A kinetic model has been assessed to examine the adsorption capability by using Lagergren linear model for PFO which would be the first-order, and characterizes the adhesion in liquid and solid arrangement depending upon the adsorption capabilities:

$$\frac{d(q_1)}{d(t)} = k_1(q_e - q_t) \quad (2)$$

where q_t is the amount of 2,4-DCP adsorbed on ionic liquid; q_e is the capacity of adsorption and k_1 is the rate constant.

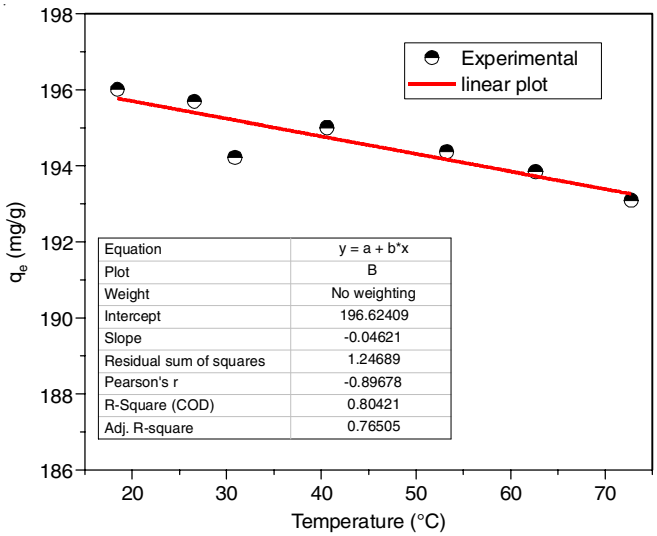

Fig. 4b. Influence of temperature in 2,4-DCP solution

Hence, the q_e is determined as 0.0558 min^{-1} and 232.68 mg g^{-1}, respectively for q_e and k_1, here R^2 is 0.9261. Fig. 5 is used to identify the model by red lines and this shows the unsatisfactory results of a pseudo first-order reaction for the adsorption [22].

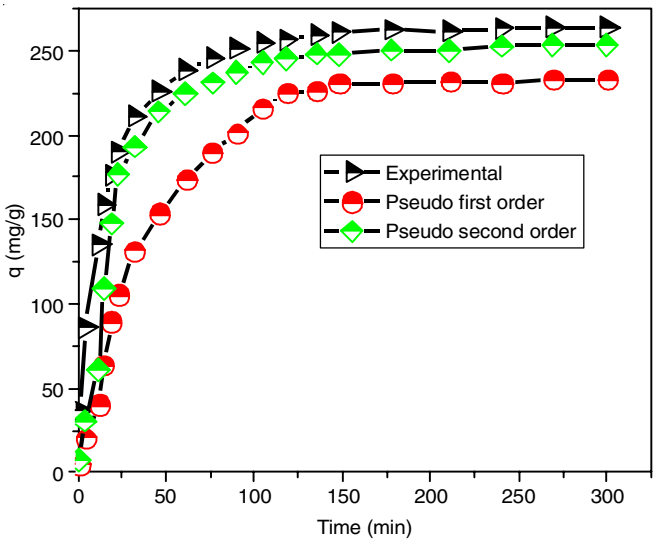

Fig. 5. Fitting of pseudo first order and pseudo second order model

Since the pseudo first-order model does not have any good relations with the experimental models, then the pseudo second-order kinetic model has been used, which is represented as follows:

$$\frac{d(q_1)}{d(t)} = k_2(q_e - q_t)^2 \quad (3)$$

where q_t is the amount of 2,4-DCP adsorbed on ionic liquid; q_e is the capacity of adsorption and k_1 is the rate constant.

Using Fig. 5, the obtained parameter values of 4.895 × 10^{-4} min^{-1} and 263.16 mg g^{-1}, respectively for q_e and k_2, and R^2 is 0.9877, which signifies successful 2,4-DCP adsorption in the ionic liquid immobilization based on phosphonium.

Weber-Morris design: The adsorbent is known to facilitate the three phases: permeation through the porous medium, intraparticle permeation as well as adsorbents on the adsorbate molecules. The Weber-Morris design simplifies the pathway explained by exterior mass transport (boundary layer diffusion) as well as surface diffusion (eqn. 3):

$$q_t = K_D t^{0.5} + C \quad (4)$$

where k_D denotes the partition correlation (mg g^{-1} $min^{1/2}$) and C is the texture of flow separation. In fact, the larger C value, the stronger the influence of the fluid layers [23].

The Weber-Morris model can be utilized to perform this experiment and divided into two phases, as shown in Fig. 6. The linear regression model is designated to the province of molecular diffusion in the first step, which is deeply engaged in the control of the adsorption process and to the steady-state stage at the moment. In the linear regression, the first step is planned when the starts to close to the origin, which indicates that the intraparticle is starting to control the stage. The R^2 value is equal to 0. 9797 in phase 1, the K_D seem to be comparable to 35.48 mg/g $min^{-1/2}$ and C to 9.031. After knowing that this phase is ruled by the adsorbed molecules the permeability might be calculated by using Weber Morris model (eqn. 5):

$$D = \frac{k_D r}{6q_e} \times \pi \quad (5)$$

where r = particle circle (cm), D = coefficient of adsorption. It was conceivable to see that they are from the same intensity when compared to the value corresponding to D, which is determined by the prototype of a pseudo-second-order model.

Isotherm studies: Three isotherm approaches *viz.* Langmuir, Freundlich and Redlich-Peterson were applied to analyze the adsorption behaviour in this study and are as follows: Langmuir′s isotherm is represented as:

$$q_e = \frac{q_{max} K_L C_e}{1 + K_L C_e} \quad (6)$$

where q_e represents the steady-state adsorption capability (mg g^{-1}), q_{max} represents the higher adsorbent capability (mg g^{-1}), and C_e represents the equilibrium state of 2,4-DCP (mg L^{-1}), and K_L represents the Langmuir constant (L mg^{-1}).

A significant characteristic of Langmuir isotherm is the assessment of the mean difference (R_L), which is defined as:

$$R_L = \frac{1}{1 + K_L C_o} \quad (7)$$

As a result, for desirable adsorbent, $0 < R_L < 1$; for undesirable adsorbent, $R_L > 1$; for regression adsorbent, $R_L = 1$; and for irrecoverable adsorbent, $R_L = 0$. The diffusion coefficient of this study was found to be 0.0231, which indicate that the process was efficient and beneficial.

Freundlich isotherm model is described as:

$$q_e = K_F C_e^{1/a} \quad (8)$$

where q_e is adsorption isotherm's ability (mg g^{-1}), K_F is sorbent strength index, C_e is an optimum concentration of 2,4-DCP and observable factor is n. According to this assertion, the process is referred to as physical adsorption.

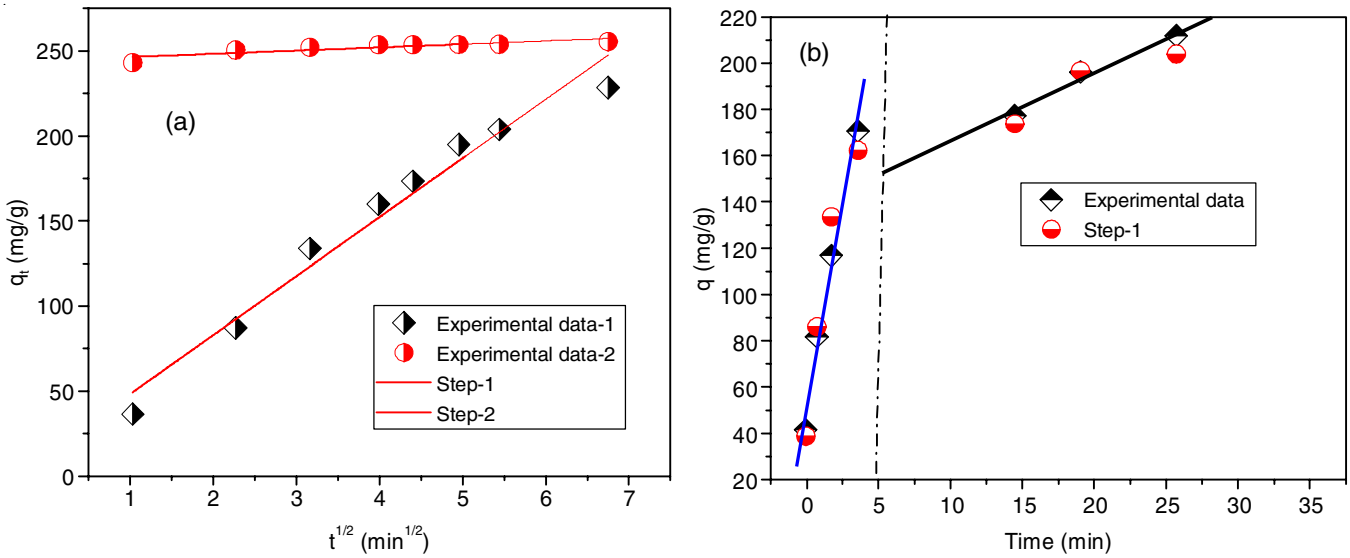

Fig. 6. Fitting of weber Morris model (a) linear plot (b) normal plot

The Redlich-Peterson model is the one that combines three parameters and is represented as follows:

$$q_e = \frac{KRP.C_e}{1+\alpha.C\beta_e} \quad (9)$$

The final concentration of 2,4-dichlorophenol ranges from 15.68 to 45.57 mg g^{-1}. Based on these findings, it is clear that capsule which are regarded as pure or original have modest adsorption rates and their capacity for adsorption will only stabilize or grow at equilibrium concentrations higher than 729 mg L^{-1}. Ionic liquid-based membranes therefore contain the ingredients needed for the phenolic compound's removal.

As shown in the adsorption experiments, the effectiveness of the membrane developed for the elimination of phenolic compounds assists in a several treatments of effluents. The variety of industrial effluent types is demonstrated by the variance in the adsorption, primarily at different temperatures and pH levels. The PSO kinetics model can be regarded as one of the suitable models because the study's findings were compared to those predicted by the Weber-Morris model, which had revealed a process restriction associated to the intraparticle diffusion.

Conclusion

This study revealed that the adsorption process of GO/Fe_3O_4@PSF entrapped in the phosphonium-based ionic liquid (trihexyltetradecylphosphonium decanoate) have the excellent capacity to remove 2,4-dichlorophenol with an efficiency of 83.33%. The treated wastewater adsorption performance was demonstrated and its kinetic attitude was verfied by using the pseudo-second-order and the Weber-Morris kinetic models. According to the Langmuir isotherm, which has adsorption capacity of 404.50 mg g^{-1}, is comparable to Redlich-Peterson isotherm, which is especially adapted to evidence with an equivalent level to one. Finally, this work can begin to contribute to the implementation of innovative strategies for treating large quantities of wastewater samples, such as membranes that can be adhered to stationary, minimizing the toxic chemical environmental impacts.

ACKNOWLEDGEMENTS

The authors are thankful to Department of Petrochemical technology, Bharathidasan Institute of Technology campus, Anna University, Tiruchirappalli, India for providing facilities and carried our research work

CONFLICT OF INTEREST

The authors declare that there is no conflict of interests regarding the publication of this article.

REFERENCES

1. M. Akhtar, M.I. Bhanger, S. Iqbal and S.M. Hasany, *J. Hazard. Mater.*, **128**, 44 (2006); https://doi.org/10.1016/j.jhazmat.2005.07.025
2. P. Antonio, K. Iha and M.E.V. Suárez-Iha, *J. Colloid Interface Sci.*, **307**, 24 (2007); https://doi.org/10.1016/j.jcis.2006.11.031
3. V. Archana, K.M. Meera S. Begum and N. Anantharaman, *Arab. J. Chem.*, **9**, 371 (2016); https://doi.org/10.1016/j.arabjc.2013.03.017
4. A. Balasubramanian, S. Venkatesan and T. Nadu, *Clean*, **42**, 64 (2014); https://doi.org/10.1002/clen.201200168
5. J.N. Hahladakis, C.A. Velis, R. Weber, E. Iacovidou and P. Purnell, *J. Hazard. Mater.*, 344, 179 (2018); https://doi.org/10.1016/j.jhazmat.2017.10.014
6. V. Marturano, P. Cerruti and V. Ambrogi, *Phys. Sci. Rev.*, **2**, 20160130 (2017); https://doi.org/10.1515/psr-2016-0130
7. C. Campanale, C. Massarelli, I. Savino, V. Locaputo and V.F. Uricchio, *Int. J. Environ. Res. Public Health*, **17**, 1212 (2020); https://doi.org/10.3390/ijerph17041212
8. K.A.M. Said, A.F. Ismail, Z.A. Karim, M.S. Abdullah and A. Hafeez, *Process Saf. Environ. Prot..*, **151**, 257 (2021); https://doi.org/10.1016/j.psep.2021.05.015
9. J. Fan, Y. Fan, Y. Pei, K. Wu, J. Wang and M. Fan, *Sep. Purif. Technol.*, **61**, 324 (2008); https://doi.org/10.1016/j.seppur.2007.11.005
10. E.O. Ezugbe and S. Rathilal, *Membranes*, **10**, 89 (2020); https://doi.org/10.3390/membranes10050089

11. W. Choi, I. Lahiri, R. Seelaboyina and Y.S. Kang, *Crit. Rev. Solid State Mater. Sci.*, **35**, 52 (2010); https://doi.org/10.1080/10408430903505036
12. H. Ahmad, Mi. Fana and D. Hui, Compos. B: Eng., 145, 270 (2018); https://doi.org/10.1016/j.compositesb.2018.02.006
13. X. Fan, G. Jiao, W. Zhao, P. Jin and X. Li, *Nanoscale*, **5**, 1143 (2013); https://doi.org/10.1039/C2NR33158F
14. S. Chong, G. Zhang, H. Tian and H. Zhao, *J. Environ. Sci*., **44**, 148 (2016); https://doi.org/10.1016/j.jes.2015.11.022
15. N. Venkatesha, P. Poojar, Y. Qurishi, S. Geethanath and C. Srivastava, *J. Appl. Phys.*, **117**, 154702 (2015); https://doi.org/10.1063/1.4918605
16. N.D. Koromilas,C. Anastasopoulos, E.K. Oikonomou and J.K. Kallitsis, *Polymers*, **11**, 59 (2019); https://doi.org/10.3390/polym11010059
17. H.T.V. Nguyen, Th.H.A. Ngo, K.D. Do, M.N. Nguyen, N.T.T. Dang, T.T.H. Nguyen, V. Vien and T.A. Vu, *Adv. Nanomater. Green Growth*, **2019**, 3164373 (2019); https://doi.org/10.1155/2019/3164373
18. C. Panisello, B. Peña, T. Gumí and R. Garcia-Valls, *J. Appl. Polym. Sci*., **129**, 1625 (2013); https://doi.org/10.1002/app.38868
19. Z. Li, M. Wu, Z. Jiao, B. Bao and S. Lu, *J. Hazard. Mater.*, **114**, 111 (2004); https://doi.org/10.1016/j.jhazmat.2004.07.014
20. C. Panisello and R. Garcia-Valls, *Procedia Eng.*, **44**, 1305 (2012); https://doi.org/10.1016/j.proeng.2012.08.764
21. K. Singh, S. Devi, H.C. Bajaj, P. Ingole, J. Choudhari and H. Bhrambhatt, *Sep. Sci. Technol.*, **49**, 2630 (2013); https://doi.org/10.1080/01496395.2014.911023
22. E. Bilgin Simsek, I. Novak, O. Sausa and D. Berek, *Res. Chem. Intermed.*, **43**, 503 (2017); https://doi.org/10.1007/s11164-016-2637-1
23. B. Xie, J. Qin, S. Wang, X. Li, H. Sun and W. Chen, *Int. J. Environ. Res. Public Health*, **17**, 789 (2020); https://doi.org/10.3390/ijerph17030789